# Immune cell complexity in the tumor microenvironment of breast cancer

Salvagno, C.

# CHAPTER 6

# hMRP8-ATTAC mice: a new model for conditional and reversible neutrophil ablation

Camilla Salvagno[1], Lisanne Raeven [1], Kim Vrijland[1], Marjolein C. Stip[1,2], Cheei-Sing Hau[1], Colin Pritchard[3], Linda Henneman[3], Rahmen Bin Ali[3], Ivo Huijbers[3], Karin E. de Visser[1,*]

[1] Division of Tumor Biology & Immunology, Oncode Institute, the Netherlands Cancer Institute, Plesmanlaan 121, 1066 CX Amsterdam, The Netherlands
[2] Current address: Immunotherapy Laboratory, Laboratory for Translational Immunology, University Medical Center Utrecht, Utrecht, Netherlands.
[3] Mouse clinic – Transgenic core facility the Netherlands Cancer Institute, Plesmanlaan 121, 1066 CX Amsterdam, The Netherlands
* Corresponding Author: Karin E. de Visser, Division of Tumor Biology & Immunology, The Netherlands Cancer Institute, Plesmanlaan 121, 1066 CX Amsterdam, The Netherlands. Phone: +31-20-5126104. Fax: +31-20-5122057. E-mail: k.d.visser@nki.nl

*Unpublished*

# Abstract

Neutrophils are not only crucial immune cells for the neutralization of pathogens during infections, but they are also key players during tumor initiation, tumor growth and metastasis formation. Several methods are available to investigate the in vivo role of neutrophils in these conditions, including depletion of neutrophils with neutralizing antibodies against Ly6G, or blockade of neutrophil recruitment with CXCR2 inhibitors. A limited number of transgenic mouse models has been generated that rely on the disruption of genes important for neutrophil development or on the injection of diphtheria toxin to induce neutrophil ablation. However, these methods have various limitations, including lack of neutrophil specificity, lack of long-term efficacy, or lack of the ability to conditionally deplete neutrophils. Therefore, we generated a transgenic mouse model for the inducible and reversible ablation of neutrophils using the ATTAC (Apoptosis Through Targeted Activation of Caspase 8) approach. With the ATTAC strategy, which relies on the expression of caspase 8-FKBP fusion protein, apoptosis is induced upon administration of a chemical dimerizer (FK506 analogue) leading to the dimerization and activation of caspase 8. In order to achieve specific neutrophil depletion, we cloned the ATTAC construct under the human migration inhibitory factor-related protein 8 (hMRP8) promotor. The newly generated hMRP8-ATTAC mice express high levels of the transgene in neutrophils and, as a consequence, dimerizer injection induces an efficient neutrophil reduction in all the organs analyzed. In contrast, no efficient neutrophil depletion was achieved in mammary tumor-bearing hMRP8-ATTAC mice, suggesting that tumor-induced neutrophil expansion prevails over dimerizer-mediated apoptosis. In conclusion, we here describe the generation and characterization of a new transgenic model for neutrophil ablation and highlight the need to improve the ATTAC strategy for the depletion of large numbers of rapidly generated short-lived cells, such as neutrophils.

## Introduction

Neutrophils are polymorphonucleated cells that have a major role in infection. Known to be the first cells to arrive at a site of inflammation, neutrophils can clear pathogens by means of several mechanisms, like phagocytosis, release of bactericidal molecules from their granules and neutrophil extracellular traps (NETosis)[1]. On top of their well-established role in infection, neutrophils are also a critical component of tumor initiation, tumor growth and metastasis formation, and both tumor-promoting and tumor-suppressing effects have been described[2]. Several cancer types, including breast cancer, are often associated with elevated numbers of circulating neutrophils and a high neutrophil-to-lymphocyte ratio (NLR) in blood predicts a worse survival[3,4]. In addition, also intratumoral neutrophils are predictive of adverse prognosis[5]. Neutrophils are constantly produced in the bone marrow under the control of granulocyte colony stimulating factor (G-CSF) and released in the circulation as terminally differentiated and mature cells[2]. The retention and the release of neutrophils in and from the bone marrow is strictly controlled by the expression of the chemokine receptors CXCR4 and CXCR2, respectively. Chemokines secreted by endothelial cells and megakariocytes like CXCL1, CXCL2 and CXCL5 are essential for the mobilization of $CXCR2^{+}$ neutrophils from the bone marrow into the circulation[2]. In cancer, both tumor and host cells can produce G-CSF which results in a strong pressure on the bone marrow to release new neutrophils, a proportion of which have an immature nuclear morphology and retain the expression of the progenitor marker cKIT[6-9]. In addition, cancer cells can express CXCR2 ligands to recruit neutrophils in the tumor microenvironment[10].

Current *in vivo* methods to study neutrophils involve either depletion of the cells or blockade of their recruitment. Neutrophils, defined as myeloid cells expressing $Ly6G^{high}Ly6C^{int}$, can be depleted using anti-Gr-1 antibodies, which recognize a shared epitope between Ly6C and Ly6G surface markers[11,12]. However, because inflammatory monocytes express high level of Ly6C, this strategy does not target only neutrophils[11]. A more specific approach is to deplete neutrophils with the anti-Ly6G antibody (clone 1A8)[11]. However, the depletion efficiency of this antibody is strongly reduced after 2 weeks of treatment, likely due to a neutralizing antibody response against the rat IgG2a antibody. Furthermore, the 1A8 antibody provides poor neutrophil depletion in C57BL/6J mice[13]. Another strategy to study the role of neutrophils in tumors is by impairing neutrophil trafficking using CXCR2-deficient mice or CXCR2 antagonists[10,14]. However, it should be considered that CXCR2 expression is not exclusive to neutrophils, but it is also expressed by other cells, including some cancer cells[15]. Recently a mouse model for the selective and inducible neutrophil depletion was developed by intercrossing $ROSA\text{-}iDTR^{KI}$ mice, which bear a Cre-inducible simian diphtheria toxin receptor (DTR), with human migration inhibitory factor-related protein 8 (hMRP8)-Cre mice, which express Cre recombinase under the control of the promoter of the neutrophil-associated S100 Calcium Binding Protein A8 (S100A8). As a result, DTR is expressed mainly in neutrophils (*hMRP8cre;ROSA-iDTR*$^{KI}$)[16]. It is known, however, that DTR systems are not ideal for long term experiments because prolonged DT injection induces an immune response against DT, annihilating its effect[17,18]. In order to overcome immunogenicity issues, we generated a novel transgenic mouse model for the

conditional and reversible ablation of neutrophils using the ATTAC (Apoptosis Through Targeted Activation of Caspase 8) approach developed by Pajvani *et al*.[19]. The ATTAC construct strategy was previously used to successfully and over prolonged periods ablate adipocytes, podocytes, pancreatic β–cells and $p16^{Ink4a}$-positive senescent cell by inducing apoptosis in these cells[19-22]. We have used the hMRP8 promotor to drive expression of the ATTAC transgene, and we here describe and characterize the hMRP8-ATTAC mouse in a non-tumor and tumor setting.

## Results

### Generation of the hMRP8-ATTAC mouse model

In order to set up a system allowing genetic depletion of neutrophils *in vivo*, we utilized the ATTAC approach in which a mutated FK506-binding-protein (FKBP) domain is fused to caspase 8[19] and expressed under control of the hMRP8 promoter. Injection of the dimerizer AP20187 induces dimerization of two FKBP domains, leading to activation of membrane-bound myristoylated caspase 8 resulting in apoptosis. An IRES-EGFP fragment was cloned after the ATTAC construct (Fig. 1A) to allow detection of transgene positive cells. The purified transgene fragment was injected in the pronucleus of FVB/N zygotes and progeny was screened for the presence of GFP. A total of 9 transgenic founders carrying the transgene were obtained, of which 3 founders showed GFP expression in circulating neutrophils with varying intensity (Fig. 1B-C). Because founder 19 had the highest GFP expression in neutrophils, we generated the hMRP8-ATTAC line from this founder mouse. Southern blot analysis of founder 19 and heterozygous progeny showed that the construct integrated in the genome in one locus as a concatemer of multiple copies (Supp. Fig. 1). Mice were bred to obtain heterozygous (HET) and homozygous (HOM) progeny. Flow cytometry analyses of several organs of HET and HOM mice showed no differences in immune cell proportion compared to wild-type (WT) mice (Supp. Fig. 2A-F, Supp. Fig. 3-5 and data not shown), indicating that the construct does not interfere with immune cell development.

### Neutrophils in hMRP8-ATTAC mice express GFP

Because S100A8 is not only expressed in neutrophils, but also in monocytes and other granulocytes[23], we set out to assess the transgenic GFP expression pattern in immune cells in hMRP8-ATTAC mice by flow cytometry analysis. Neutrophils showed GFP expression in all the organs analyzed, *i.e.* blood, spleen, lung, liver and lymph node, of HET hMRP8-ATTAC mice (Fig. 2A-E). In line with the double number of transgene copies, neutrophils in HOM mice displayed a more intense GFP expression (Fig. 2A-E). Further analyses of other myeloid cell populations showed a minimal expression of GFP in eosinophils and monocytes of HOM hMRP8-ATTAC mice compared to WT mice (Supp. Fig. 6A-E). These levels were much lower than the GFP levels of neutrophils (Fig. 2F). Dendritic cells and resident macrophages, like red pulp macrophages in the spleen, Kupffer cells in the liver, alveolar macrophages in the lung and the $CD169^+$ macrophages in the lymph node, were GFP negative (Supp. Fig. 6A-E). As expected, also $CD3^+$ T cells did not express GFP (Supp. Fig. 6A-D).

We next set out to investigate at which stage of hematopoietic differentiation

(Fig. 3A) the ATTAC construct was expressed. By flow cytometry analysis of bone marrow cells from HET and HOM hMRP8-ATTAC mice, we observed that Lineage$^-$ Sca1$^+$cKIT$^-$ (LSK), common myeloid progenitors (CMP) and megakaryocyte erythroid progenitor (MEP) were GFP negative (Fig. 3B and Supp. Fig. 7A). Along the line of neutrophil differentiation, we observed a modest increase in GFP expression, albeit not significant, in granulocyte monocyte progenitor (GMP), which intensified in promyelocytes and even more in neutrophils (Fig. 3B and Supp. Fig. 7A). A small increment in GFP expression was also seen in monocyte dendritic cell progenitor (MDP) and monocytes (Fig. 3B and Supp. Fig. 7A), in line with previous data showing modest GFP expression in monocytes in several organs (Supp. Fig. 6A-E). Altogether, these data indicate that the hMRP8 promoter becomes active in the promyelocytes and MDP populations, inducing transgene expression in these cells and in the following differentiated populations.

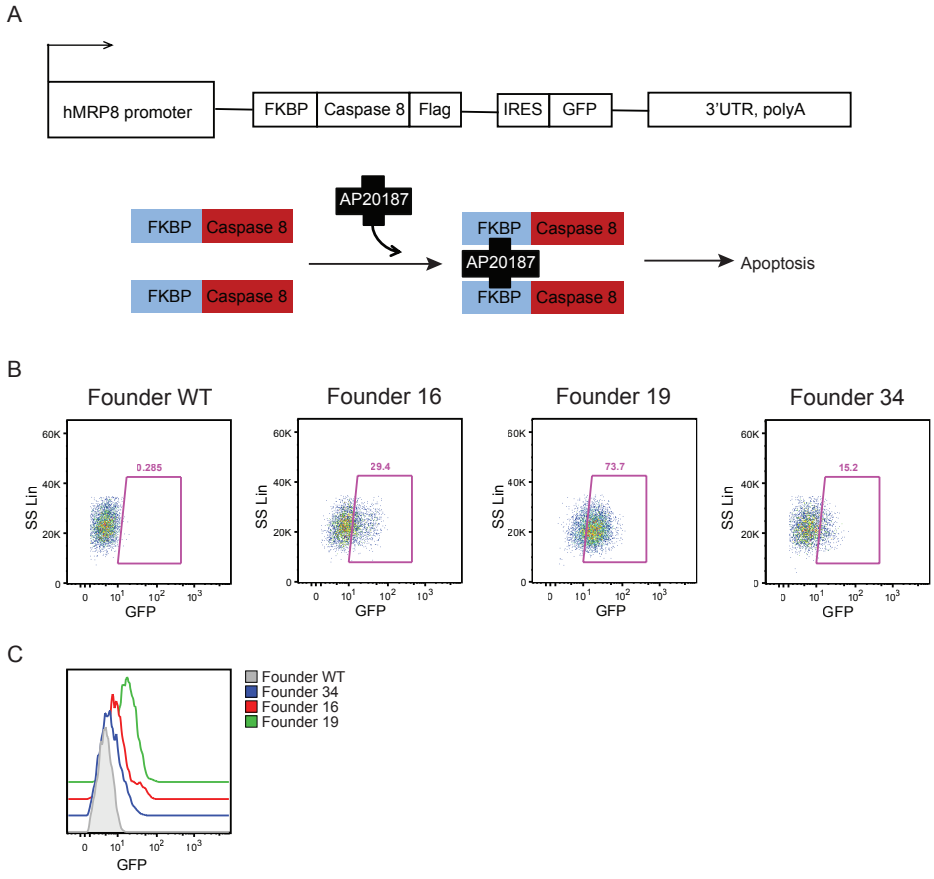


**Fig. 1 | Generation of hMRP8-ATTAC mice.** (A) Schematic representation of the ATTAC construct and the mechanism of apoptosis induced by the dimerizer AP20187. (B-C) Dot plots and histograms showing GFP expression in circulating neutrophils of four hMRP8-ATTAC founders as determined by flow cytometry. One of the founders does not carry the transgene as detected by PCR (Founder WT), the other three carry the transgene and express GFP at different levels (Founders 16, 19, 34).

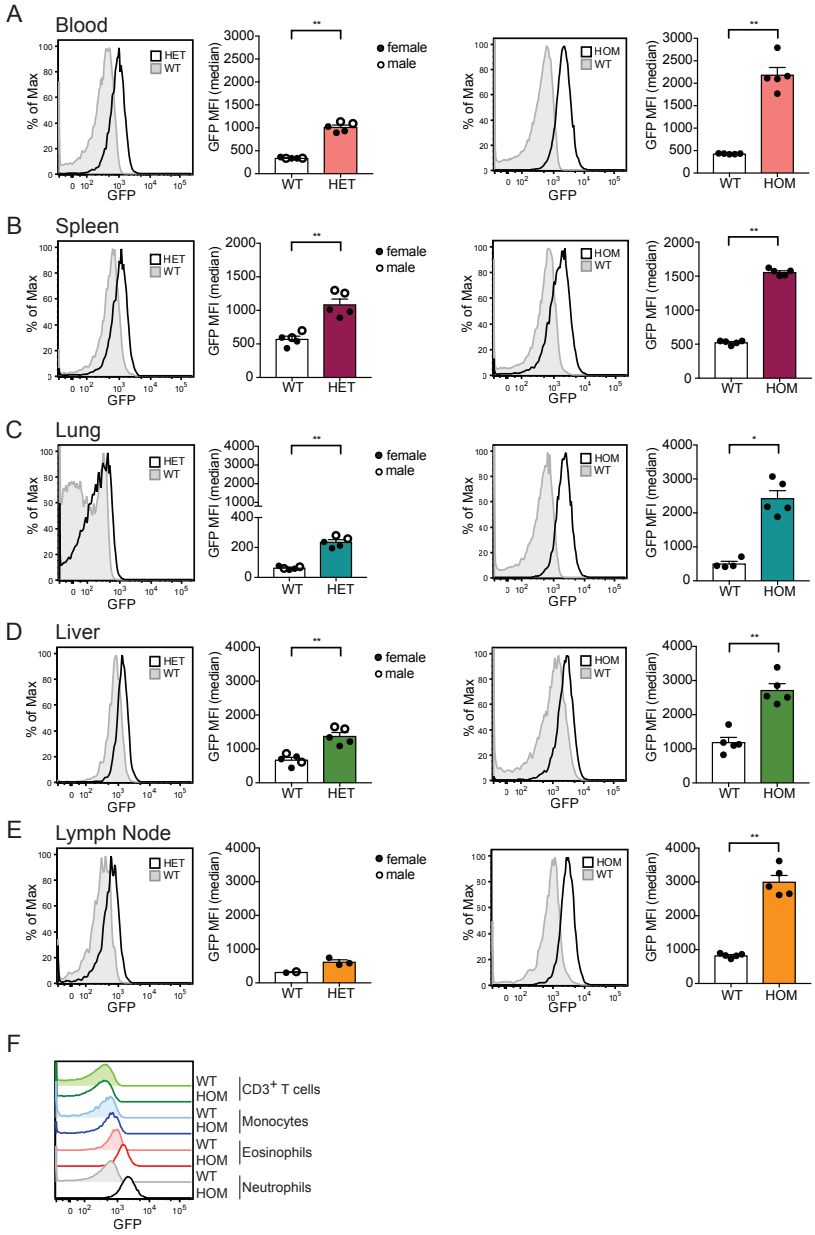


**Fig. 2 | Neutrophils in the hMRP8-ATTAC mouse model express the transgene.** (A-E) Representative histograms of GFP expression and quantification of the Median Fluorescence Intensity (MFI) of GFP in neutrophils from blood, (A), spleen (B), lung (C), liver (D) and lymph node (E) of heterozygous (left) and homozygous (right) hMRP8-ATTAC mice (n=3-5) compared to WT littermates (n=2-5), as determined by flow cytometry. Open circles represent male hMRP8-ATTAC mice and closed circles represent female hMRP8-ATTAC mice. (F) Representative histogram comparing GFP expression levels in circulating neutrophils, eosinophils, monocytes and $CD3^+$ T cells of homozygous hMRP8-ATTAC mice and WT littermates. WT, wild type; HET, heterozygous; HOM, homozygous. Data presented in A-E are mean values ± SEM. *$p < 0.05$, **$p<0.01$ by Mann–Whitney test.

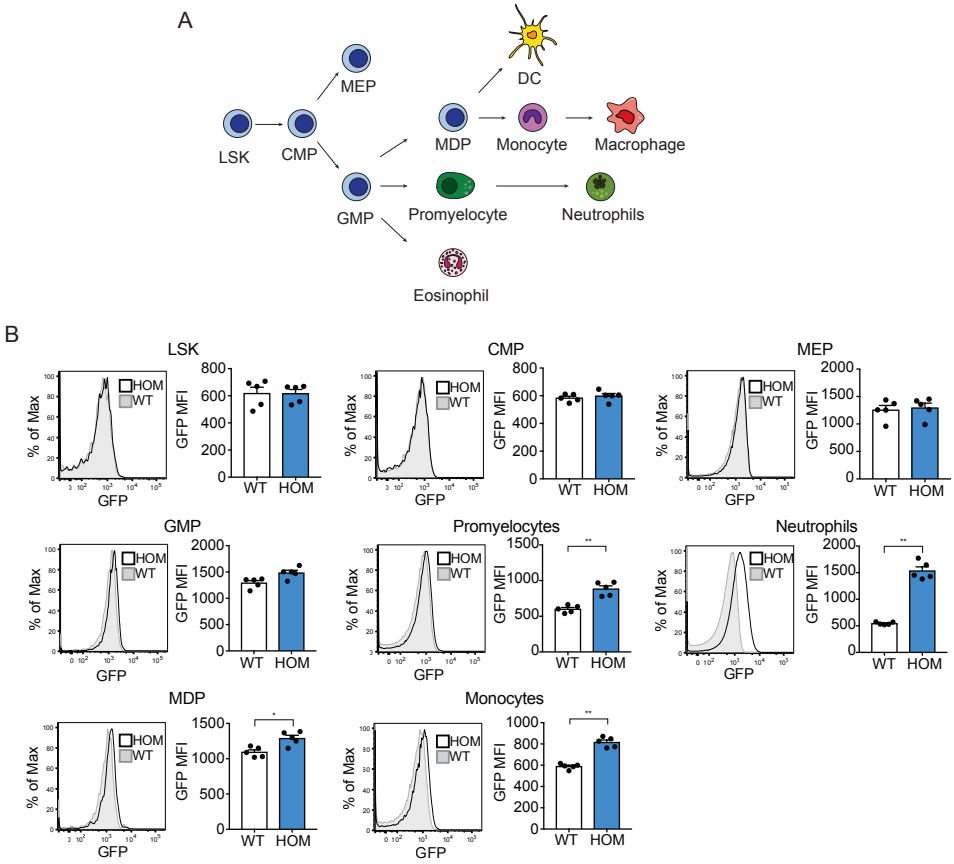


**Fig. 3 | The ATTAC transgene starts to be expressed at the GMP level in the bone marrow.** (A) Schematic representation of the hematopoietic tree. (B) Representative histograms of GFP expression and quantification of the Median Fluorescence Intensity (MFI) of GFP in different hematopoietic cell populations depicted in (A) in the bone marrow of homozygous female hMRP8-ATTAC mice and WT littermates (n=5/group), as determined by flow cytometry. WT, wild type; HOM, homozygous. LSK, Lineage$^-$SCA1$^+$Kit$^-$; CMP, common myeloid progenitor; MEP, megakaryocyte-erythroid progenitor; GMP, granulocyte-macrophage progenitor; MDP, monocyte/macrophage-dendritic cell progenitor. Data presented in B are mean values ± SEM. *p < 0.05, **p<0.01 by Mann–Whitney test.

**Depletion of neutrophils in the hMRP8-ATTAC mouse model upon dimerizer injection**

Because HOM hMRP8-ATTAC mice showed a stronger transgene expression, we continued to evaluate the functional activity of the construct in these mice. In order to test the depletion specifically of transgene-expressing cells, we injected hMRP8-ATTAC and non-transgene-carrying control WT mice with the dimerizer AP20187 every day for a week (Fig. 4A). Two days of dimerizer treatment resulted in a reduction of circulating neutrophils in hMRP8-ATTAC mice and not WT mice, while monocytes and eosinophils were not affected (Fig. 4B-C and Supp. Fig. 8A). Interestingly, a slight decrease in neutrophils was observed in the control groups (vehicle-treated hMRP8-ATTAC and vehicle/dimerizer-treated WT mice) compared to pre-treatment samples (Fig. 4B-C and Supp. Fig. 8A), probably due to fluctuation in experimental conditions between time points. After a week of dimerizer treatment, neutrophils were strongly reduced in blood and lungs and modestly in spleen and bone marrow of hMRP8-ATTAC mice with a concomitant small, but significant, relative increase in monocytes in all the organs (Fig. 4D-E). The frequency of eosinophils was not influenced by the dimerizer treatment, except for a reduction in pulmonary eosinophils (Fig. 4F). Tissue resident macrophages in the spleen and lung were not affected (Fig. 4G). We observed a small increase in circulating neutrophils and monocytes, but not in eosinophils and resident macrophages, in WT mice after dimerizer injection, probably due to a modest inflammatory response against the compound (Supp. Fig. 8B-E). Overall, these data illustrate that, in line with the GFP expression profile, neutrophils are most efficiently depleted in all analyzed organs and circulation upon dimerizer inoculation. Other immune cell populations are minimally affected.

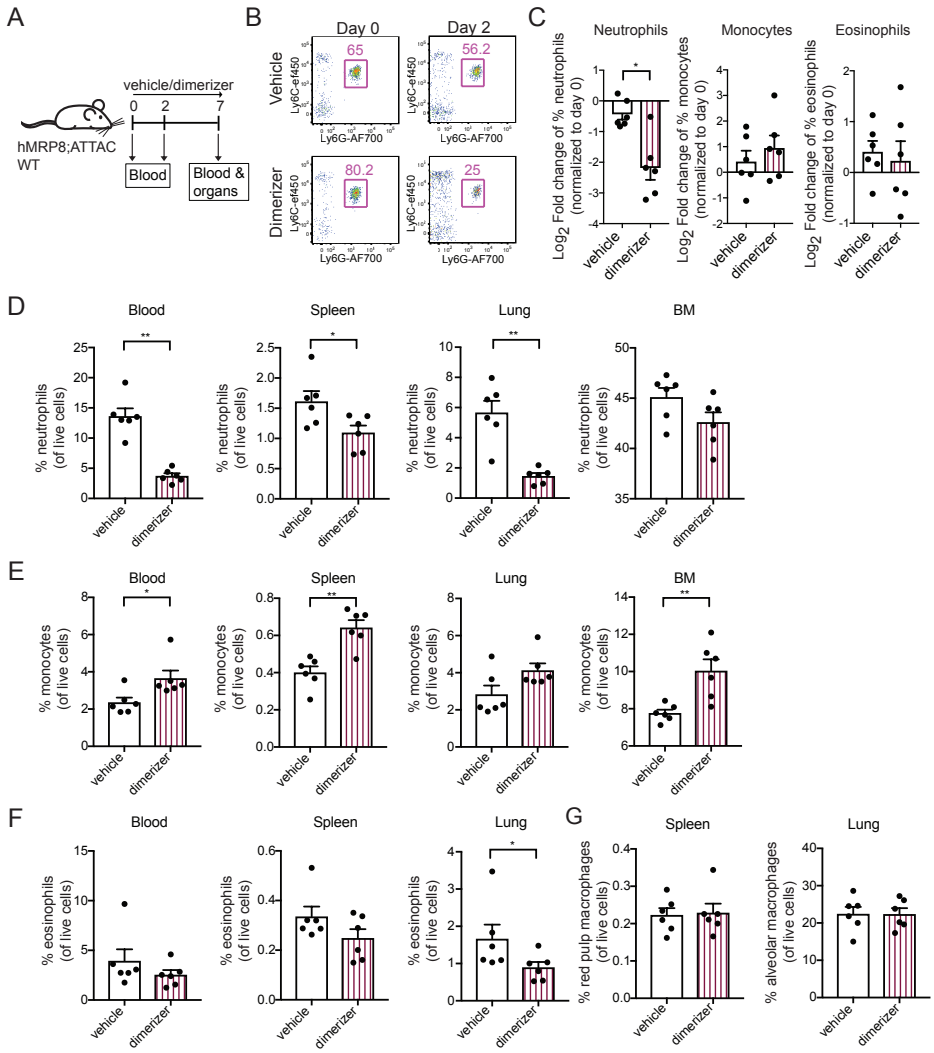


**Fig. 4 | Dimerizer treatment reduces neutrophil frequency in hMRP8-ATTAC mice.** (A) Schematic representation of the experimental design. Homozygous hMRP8-ATTAC or age-matched WT female mice were treated daily with vehicle or dimerizer for 7 consecutive days. Blood was analyzed by flow cytometry before the start of the treatment and two days after the start of the treatment. At the seventh day, mice were sacrificed and tissues were processed and analyzed by flow cytometry. (B) Representative dot plots showing percentages of neutrophils (of $CD11b^{+}Siglec\ F^{-}$ cells) in the blood of either vehicle- or dimerizer-treated hMRP8-ATTAC mice before and after two days of treatment. (C) $Log_2$ fold change of circulating neutrophils, monocytes and eosinophils defined as % of live two days after treatment compared to day 0 in hMRP8-ATTAC mice (n=6/group). Fold change was calculated by dividing the frequency of neutrophil at day 2 by the frequency of neutrophils at day 0. (D-G) Frequencies of neutrophils (D), monocytes (E), eosinophils (F) and resident macrophages (G) in blood, spleen, lung and bone marrow of hMRP8-ATTAC mice (n=6/group) treated with vehicle or dimerizer for seven consecutive days. Data presented in C-G are mean values ± SEM. *p < 0.05, **p<0.01 by Mann-Whitney test.

**Dimerizer treatment does not reduce neutrophils in tumor-bearing hMRP8-ATTAC mice**

We and others have reported previously that neutrophils accumulate in several organs of tumor-bearing mice and that their expansion is related to primary tumor size[2,6,7]. In order to investigate the depletion efficacy of neutrophils in the hMRP8;ATTAC model in a tumor setting, we transplanted mammary tumor pieces, derived from the transgenic *K14cre;Cdh1$^{F/F}$;Trp53$^{F/F}$* (KEP) mouse mammary tumor model[24,25], in the mammary fat pad of syngeneic mice. Vehicle or dimerizer treatment started at a tumor size of 25mm$^2$ and continued until the tumor size reached the humane end-point (225mm$^2$) (Fig. 5A). As a positive control, we treated a group of hMRP8-ATTAC mice with the neutralizing antibody against Ly6G (clone 1A8) that was previously used in our studies to deplete neutrophils[7]. In line with the finding that neutrophils do not have an impact on primary KEP tumor outgrowth[7], treatment of tumor-bearing hMRP8-ATTAC mice with either anti-Ly6G or dimerizer did not influence the tumor-specific survival compared to vehicle-treated mice (Supp. Fig. 9A). The frequency of circulating neutrophils was increased at a tumor size of 100mm$^2$ in vehicle-treated mice when compared to baseline levels at a tumor size of 25mm$^2$ (Fig. 5B). As expected, neutrophil levels were reduced in anti-Ly6G-treated tumor-bearing mice (Fig. 5B). In contrast, dimerizer treatment did not reduce neutrophils in the circulation at the same tumor size (Fig. 5B). Circulating monocytes expanded with tumor growth in anti-Ly6G- and dimerizer-treated mice while the frequency of eosinophils modestly increased in anti-Ly6G-treated mice compared to vehicle-treated mice at a tumor size of 100 mm$^2$ (Fig. 5C-D). Prolonged dimerizer treatment did not reduce neutrophil levels in the blood and in the other organs, including the tumor, when mice were analyzed at end-stage (Fig. 5E-H; Supp. Fig. 10). As anticipated, while short-term anti-Ly6G treatment reduced circulating neutrophils (Fig. 5B), this effect was lost over time as no differences were observed in the proportion of neutrophils in the blood of end-stage mice (Fig. 5E); yet, a significant increase in neutrophil accumulation was observed in the spleen, possibly because of the appearance of emergency granulopoiesis, triggered by neutrophil depletion, in this organ (Fig. 5E). Monocyte levels were increased in all tissues analyzed after dimerizer treatment, while the proportion of eosinophils did not change, except for a slight decrease in the blood of dimerizer-treated mice (Supp. Fig. 9B-C and Supp. Fig. 10). A modest reduction in CD3$^+$ T cells was also observed in lungs after dimerizer treatment (Supp. Fig. 9D). In addition, spleen and lung resident macrophages and tumor-associated macrophages (TAMs) were not affected by the treatment (Supp. Fig. 9E). Because inflammation can induce S100A8 upregulation in endothelial cells[26], we counted the number of CD31$^+$ vessels in the tumor of dimerizer-treated hMRP8-ATTAC mice. No difference in vessel density was observed upon dimerizer administration, suggesting that KEP tumors do not activate the hMRP8 promotor in endothelial cells (Fig. 9F).

These data show that, although dimerizer treatment was effective in reducing neutrophils in a homeostatic situation (Fig. 4), it was not successful in a cancer setting, probably due to the high cancer-induced pressure for neutrophil production on the bone marrow.

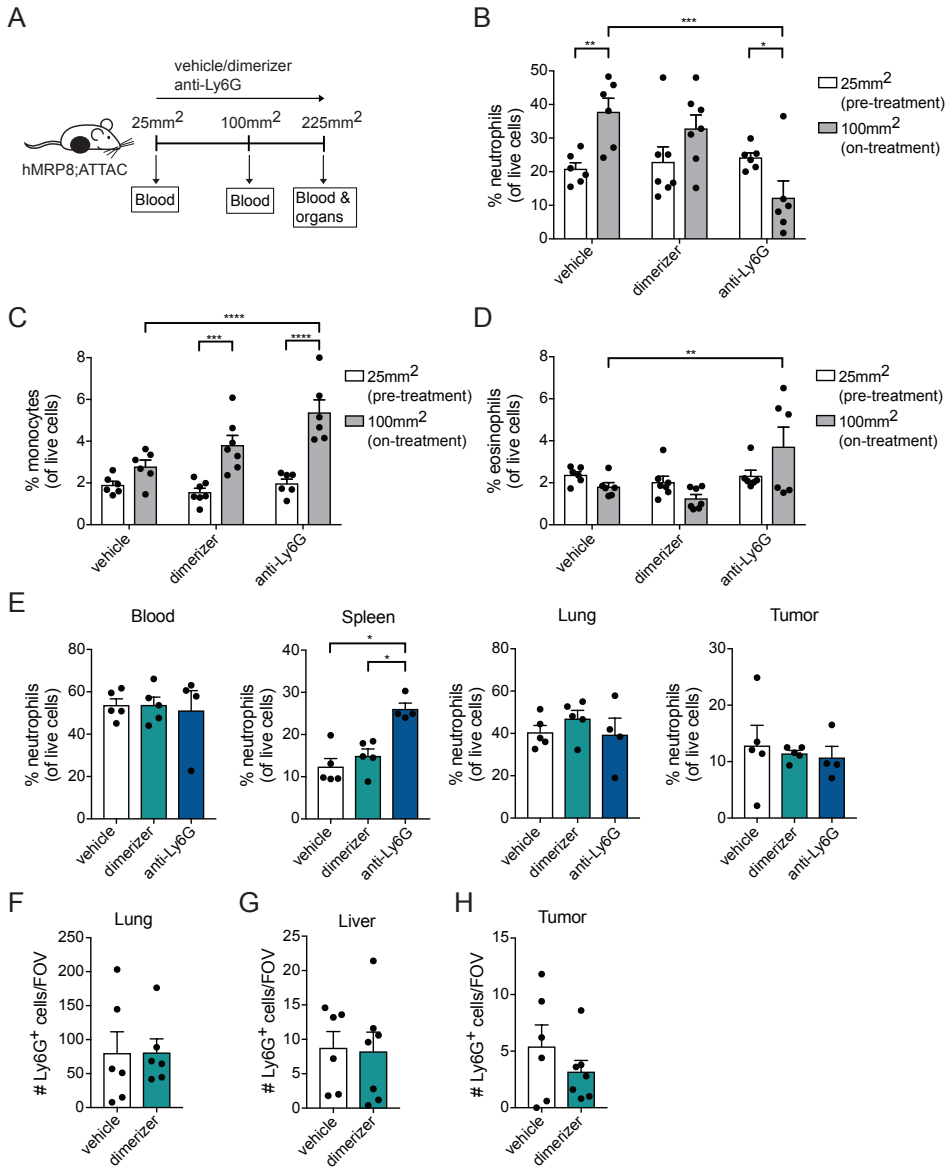


**Fig. 5 | Dimerizer treatment does not reduce neutrophil frequency in tumor-bearing hMRP8-ATTAC mice.** (A) Schematic representation of the experimental design. Female homozygous hMRP8-ATTAC mice were orthotopically transplanted in the mammary fat pad with *K14cre;Cdh1*$^{F/F}$*,Trp53*$^{F/F}$ tumor fragments. Mice were treated with either vehicle, dimerizer or anti-Ly6G until they were sacrificed when the tumor size reached 225mm$^2$. Blood was collected before the start of the treatment (25mm$^2$) and at a tumor size of 100mm$^2$. (B-D) Frequency of neutrophils (B), monocytes (C) and eosinophils (D) in the blood of hMRP8-ATTAC mice treated as indicated (vehicle and anti-Ly6G treatments, n=6/tumor size; dimerizer treatment, n=7/tumor size) at a tumor size of 25mm$^2$ and 100mm$^2$, as determined by flow cytometry. (E) Frequency of neutrophils in blood, spleen, lung and tumor of end-stage hMRP8-

ATTAC mice (n=4-5) as determined by flow cytometry. (F-H) Quantification of Ly6G$^+$ cells in viable areas of lung (F), liver (G) and tumor (H) of end-stage hMRP8-ATTAC mice (n=6-7) as determined by IHC. Values represent average number of positive cells per field of view (FOV) quantified by counting five high-power microscopic fields per tumor. Data presented in B-D are mean values ± SEM. *p < 0.05, **p<0.01, ***p<0.001, ***p<0.0001 by two-way ANOVA with Sidak's multiple comparisons test. Data presented in E-H are mean values ± SEM. *p < 0.05 by Mann–Whitney test.

## Discussion

As one of the first immune cells that arrive into an inflamed area, neutrophils represent an indispensable component to fight infections. Recent studies have also shown that they are not only important against pathogens, but they also play a critical role in tumor progression and metastasis formation, with both pro- and anti-tumoral functions being discovered[2]. In order to investigate the functional contribution of neutrophils to specific inflammatory stimuli, infections or cancer, it is desirable to deplete or inhibit these cells and monitor the consequences. Thus far, the most commonly used *in vivo* strategies to ablate neutrophils are treatment with the depleting anti-Ly6G and anti-Gr1 antibodies and the use of CXCR2 antagonists to interfere with neutrophil trafficking. However, the short-term efficacy of anti-Ly6G, its inefficiency at depleting neutrophils in C57BL/6J mice and the non-specificity of anti-Gr1 and CXCR2 antagonists are the main concerns[11,13,15]. In addition, several genetic models have been generated. For example, the *LysMcre;Mcl-1$^{F/F}$* model is deficient in the anti-apoptotic molecule Mcl-1, a Bcl-2 family member, in neutrophil and monocyte/macrophage populations[27]. This mouse model shows decreased numbers of neutrophils, while macrophage levels were not influenced because of a compensatory upregulation of other Bcl-2 family members[27]. Others have used mice bearing point mutations in or full knock-out of the growth factor independence 1 (Gfi1), which is important for neutrophil and T cell development[28,29]. In addition, since G-CSF is the main growth factor for neutrophil development, G-CSF$^{-/-}$ mice display neutropenia and deficiency in granulocyte and macrophage progenitors[30]. Although these models are characterized by a decrease in neutrophil levels, they do not allow to conditionally induce or revert neutrophil depletion. Furthermore, other concerns of the aforementioned genetic models are that they may have unknown developmental defects, or may have developed compensatory mechanisms to cope with the absence of neutrophils or, since neutrophils are critical for immune defense, may have a different composition of the host microbiome. Recently another mouse model for neutrophil ablation was developed by intercrossing ROSA-iDTR$^{KI}$ mice, which bear a Cre-inducible simian diphtheria toxin receptor (DTR), with hMRP8-Cre mice to induce DTR expression (*hMRP8cre;ROSA-iDTR$^{KI}$*) in S100A8-expressing cells[16]. It is known, however, that long-term treatment with DT induces an immune reaction against the compound itself, blocking its effect[17,18]. There is a clear need for genetic models that allow for long-term efficient and specific conditional and reversible neutrophil depletion. We here describe a novel transgenic mouse model for neutrophil depletion that relies on the activation of caspase 8-FKBP fusion protein upon injection with a chemical dimerizer. The hMRP8-ATTAC mouse model shows a striking hMRP8 promotor activity in neutrophils and a much lower activity in monocytes and eosinophils, as defined by GFP expression in these cells. In the

bone marrow, the transgene is expressed at very low levels at the GMP stage and is upregulated during differentiation along the monocytic and granulocytic lineages. Importantly, because S100A8 expression is downregulated during differentiation into macrophages and DCs[31,32], we did not observe GFP expression in these cells. As expected, because of their high transgene expression, neutrophils in the hMRP8-ATTAC model are very sensitive to the effects of the dimerizer, resulting in a decreased frequency of these cells in blood, lung and spleen, and to a lesser extent in the bone marrow. Future experiments will evaluate if neutrophil depletion is also achieved after long-term treatment with the dimerizer. Although the dimerizer treatment reduces neutrophil levels in this mouse model, it fails to do so in tumor-bearing hMRP8-ATTAC mice. Several reasons might be responsible for the lack of neutrophil depletion in tumor-bearing hMRP8-ATTAC mice. First, it is well established that tumors stimulate granulopoiesis in the bone marrow and release immature and mature neutrophils into the circulations[2,6-8]. Thus, in chronic inflammatory conditions, like in tumor-bearing hosts, neutrophils are constantly produced in excessive amounts, thus perhaps exceeding the activity of the dimerizer. Secondly, the half-life of the dimerizer is approximately 5 hours (Takara Bio Inc.) and because we injected it only once a day, it is probably not frequent enough to suppress the continuous tumor-induced neutrophil expansion. Thirdly, neutrophils are quickly replenished after they die[2,33]. Indeed, previous studies using the ATTAC system aimed at depleting adipocytes, podocytes, pancreatic β–cells and $p16^{Ink4a}$-positive senescent cells showed a pronounced and long-lasting depletion of these cells[19-22,34]. Although these studies used even a lower concentration of the dimerizer per injection compared to our study, these cells are not renewed at the same rate as neutrophils, likely explaining the more stable depletion. Frequent dimerizer injections for the tumor-bearing hMRP8-ATTAC model might be a solution, or future studies should aim at increasing dimerizer half-life or at developing a formulation of the dimerizer that remains stable in the animals' chow. As for the DT in the *hMRP8cre;ROSA-iDTR$^{KI}$* mouse, the dimerizer might be immunogenic and trigger a neutralizing antibody-mediated response. However, others have performed long dimerizer treatment for 4 weeks[19] and even for 4 months[34] in immunoproficient mice resulting in efficacious cell depletion, suggesting that the dimerizer does not elicit an immune response.

Importantly, in a cancer setting, inflammation can induce S100A8 upregulation. For example, tumor-derived VEGF-A, TGFβ and TNFα may induce S100A8 expression in macrophages and endothelial cells[26] or monocyte/macrophage-derived factors may stimulate its expression in cancer cells[35]. However, in tumor-bearing hMRP8-ATTAC mice, we did not observe loss of TAMs or endothelial cells upon dimerizer treatment, suggesting that in this context these cells do not upregulate the transgene. Moreover, because in this tumor model we transplanted a *K14cre;Cdh1$^{F/F}$;Trp53$^{F/F}$* tumor fragment that does not carry the ATTAC transgene, the dimerizer could not affect directly cancer cells.

Interestingly, differently from the *hMRP8cre;ROSA-iDTR$^{KI}$* mice, monocyte proportions modestly increase in several tissues of non-tumor-bearing hMRP8-ATTAC and WT mice and tumor-bearing hMRP8-ATTAC upon dimerizer injection. Most likely, this is just a relative increase in monocytes due to neutrophil reduction or an increment in their absolute number due to dimerizer-mediated stimulation of

myelopoiesis. Indeed, we observed a higher proportion of monocytes in the bone marrow of dimerizer-treated hMRP8-ATTAC mice. Interestingly, a similar increase in monocytes was also observed in the Gfi1 mutated and knock-out models[28,29]. Future experiments should aim at evaluating the absolute number of myeloid cells upon dimerizer injection.
In conclusion, we here describe the generation and characterization of a new mouse model for the conditional ablation of neutrophils. Although successful conditional induction of apoptosis in neutrophils through the activation of caspase 8 is achieved in hMRP8-ATTAC mice, future studies should focus on improving the model in order to sustain neutrophil depletion in a chronically inflamed context.

## Acknowledgments

This work was supported by the European Research Council (ERC consolidator award INFLAMET 615300), European Union (FP7 MCA-ITN 317445 TIMCC) and Oncode. We thank the mouse clinic – transgenic core facility, flow cytometry facility, the animal facility and the animal pathology facility at the Netherlands Cancer Institute. We thank Philipp Scherer (the University of Texas Southwestern Medical Center, Dallas) and Massimiliano Mazzone (VIB-KU, Belgium) for providing us with reagents.

## Author contributions

C.S. and K.E.dV conceived the ideas and designed the experiments. C.P., R.B.A., L.H. and I.H generated the hMRP8-ATTAC mice. C.S., L.R., K.V., M.C.S., and C-S.H. performed the experiments and analyzed the data. C.S. and K.E.dV wrote the paper.

## Competing financial interests

The authors declare no competing financial interests.

## Methods

**Generation of hMRP8-ATTAC transgenic mice**
hMRP8-ATTAC mice were generated in the animal laboratory facility of the Netherlands Cancer Institute by the Mouse clinic – Transgenic core facility. The hMRP8-ATTAC transgenic construct was designed as follows. The FKBP-Caspase8 fragment was subcloned from the POD-ATTAC construct[21] (kindly provided by P. Scherer, the University of Texas Southwestern Medical Center, Dallas) and inserted into a pRRL2 vector containing the humanMRP8 (hMRP8) promoter and hMRP8 3' untranslated region[36] (a gift from M. Mazzone, VIB-KU, Belgium). An IRES-EGFP fragment was inserted at 3' of the ATTAC construct. The fragment containing the hMRP8 promoter, FKBP-Caspase8 fusion protein, and the 3' untranslated region was released by ClaI and PspXI digestion, purified from agarose gel by electroelution and microinjected in the pronucleus of FVB/N zygotes. Progenies were screened for GFP by PCR on toe clip-derived genomic DNA (forward: 5'– CTGGACGGCGACGTAAACGGC

– 3'; reverse: 5'– TCCTTGAAGAAGATGGTGCG – 3'). A total of 9 founders were obtained carrying the transgene, and 3 of them showed GFP expression in circulating neutrophils as assessed by flow cytometry.
Heterozygous hMRP8-ATTAC mice were maintained in breeding with FVB/N mice, obtained from Janvier, (HET x FVB/N) to obtain HET and WT mice. Offspring was genotyped by lysing toe clips from the mice in Direct PCR tail (Viagen) containing 1% proteinase K (Sigma Aldrich) and subsequent PCR for the hMRP8 promoter (forward: 5'– CACCACAGTCTTCAAGGTTG – 3'; reverse: 5'– GGCCATACATCCCTGAAACTGA – 3'). After crossing two heterozygous mice to obtain homozygous mice, the colony was maintained by breeding two homozygous mice (HOM x HOM). Genotyping was performed by quantitative RT-PCR for the *Egfp* gene on toe clip lysate. The TaqMan Copy Number Reference Assay for the mouse *Tfrc* gene (Thermo Fisher) was used as the endogenous reference gene. This reference, DNA (5ng/µl), GFP-specific primers (forward: 5' - GAAGCGCGATCACATGGT - 3'; reverse: 5' - CCATGCCGAGAGTGATCC - 3') (Invitrogen) and GFP probe (UPL 67, Roche) were added to TaqMan Universal Mastermix (Thermo Fischer) and the RT-PCR was run on a StepOnePLus PCR system. The copy number of the construct in the mice was calculated using the comparative threshold cycle (CT) method, using a sample containing a single GFP copy as a reference.

**Materials and animals**
The chemical dimerizer AP20187 was diluted in ethanol according to manufacturer's recommendation (Takara Bio Inc.) before injection. Dimerizer or vehicle (ethanol) was diluted in water containing 2% Tween and 10% PEG-400 (Sigma Aldrich) and was injected i.p. every day for a week at a dose of 0,5µg/g body weight in homozygous female hMRP8-ATTAC mice (age 17-19 weeks-old) and age-matched female FVB/N mice. Blood was collected before the start of the treatment and after two days by tail vein puncture.
For tumor transplantation experiments, donor tumors from KEP mice[24] were collected in ice-cold PBS, cut in small pieces and resuspended in Dulbecco's Modified Eagle's Medium F12 containing 30% fetal calf serum and 10% dimethyl sulfoxide and stored at −150 °C. At the day of transplantation, KEP tumor pieces were thawed and tumor pieces (1x1 mm) were orthotopically transplanted into the mammary fat pad of 8-13 weeks-old hMRP8-ATTAC female mice. Mice were palpated three times a week and the perpendicular tumor diameters of mammary tumors were measured twice a week using a caliper. Treatment with vehicle, dimerizer or anti-Ly6G (single loading dose of 400 µg followed by 100 µg three times a week, clone 1A8, BioXCell) started at a tumor size of 25mm$^2$ and continued until the tumor reached 100mm$^2$ when the mice were sacrificed. Blood was collected before the start of the treatment and at a tumor size of 100mm$^2$ by tail vein puncture.
Mice were kept in individually ventilated cages at the animal laboratory facility of the Netherlands Cancer Institute. Food and water were provided ad libitum. Animal experiments were approved by the Animal Ethics Committee of the Netherlands Cancer Institute and performed in accordance with institutional, national and European guidelines for Animal Care and Use.

**Southern Blot**
Genomic DNA was isolated from tissue by proteinase K lysis and organic extraction with phenol-chloroform. Southern blot analysis was performed using 10 µg genomic DNA, digested with EcoRV to determine the status of transgene integration. Blotting and hybridization was performed as described previously[37]. Primers for amplification of the GFP probe are the following: forward primer 5'-CCA TGG TGA GCA AGG GCG AGG AGC TG-3'; and reverse primer 5'-CCT TGT ACA GCT CGT CCA TGC CGA GA-3'. The GFP probe was radioactively labeled using Random primers DNA labeling kit (Thermo Fisher Scientific). Hybridization of the GFP probe to EcoRV-digested DNA resulted in a concatemer band of 6114 kb.

**Flow cytometry**
Tumor, spleen, liver, lung, lymph nodes and bones were collected in ice-cold PBS, while blood was collected in heparine or in EDTA-coated tubes (for tail vein puncture). Tumors were mechanically chopped using the McIlwain Tissue Chopper (Mickle Laboratory Engineering) as described[38], while spleen, liver and lungs were minced using a scalpel. Subsequently, tumor, spleen and liver were digested in serum-free DMEM containing 3mg/mL Collagenase A (Roche) and 25µg/mL DNAse (Sigma Aldrich), while lungs were digested in serum-free DMEM containing 100µg/mL TM Liberase (Roche) and 25µg/mL DNAse. After 30min for spleen, lung and liver and 1hour for tumors, digestion was inactivated by adding DMEM containing 8% FCS and P/S. Samples were then filtered through a 100µm cell strainer. Lymph nodes were cut manually, digested in serum-free RPMI containing 100µg/mL TL Liberase (Roche) and 25µg/mL DNAse for 30 min, inactivated in RPMI containing 8% FCS, P/S and β-mercaptoethanol and filtered through a 100µm cell strainer. Bone marrow cells were flushed out from humeri and tibiae and filtered through a 100µm cell strainer. Erythrocytes were lysed using a NH4Cl buffer (155mM NH4Cl, 10mM KHCO3, 0.1mM EDTA) on the lungs, spleen, liver, blood and bone marrow. Cells were then washed using FACS buffer (PBS containing 0.5% BSA and 2mM EDTA) and counted with TC20 Automated Cell Counter (Bio-rad).
$3*10^6$ cells of the single cell suspensions were seeded in a 96-well plat and stained with antibodies for flow cytometry analysis. Briefly, all cells except BM cells, were incubated in Fc block (BD, clone 2.4G2) diluted 1:50 in FACS buffer for 5min. Cells were then stained with fluorochrome-conjugated antibodies (Supplementary Table 1) for 20 min at 4°C in the dark in FACS buffer. 7AAD (1:20; eBioscience) was added to exclude dead cells. Acquisition was performed on a BD LSRII flow cytometer using Diva Software (BD Biosciences) and data analysis was performed using FlowJo software version 9.9.6.
To determine the reduction of neutrophils after dimerizer treatment, the % of circulating neutrophils (of live cells) at day 2 was divided by the % of circulating neutrophils at day 0. $Log_2$ was consequently calculated.

**Immunohistochemistry**
All immunohistochemical analyses were performed by the Animal Pathology facility at the NKI, Amsterdam. Tissues were fixed for 24 h in 10% neutral buffered formalin and embedded in paraffin. 5 µm thick paraffin sections were cut, deparaffinized and antigen retrieval was performed with Proteinase K. Samples were then stained with

anti-Ly6G antibody (clone 1A8, BD Biosciences, 1:150) or CD31 (polyclonal, Abcam, 1:200). Quantification of positive cells was performed manually by counting five high-power (40x) fields of view (FOV) per tumor. Samples were visualized with a BX43 upright microscope (Olympus) and images were acquired in bright field using cellSens Entry software (Olympus).

**Statistical analysis**

Statistical analyses were performed using GraphPad Prism 7 (GraphPad Software Inc., La Jolla, CA). The two-tailed Mann-Whitney test was used for immunohistochemistry and flow cytometry analysis. Where indicated, two-way ANOVA with Sidak's multiple comparison test was used. P values $< 0.05$ were considered statistically significant.

## References


1. Nathan, C. Neutrophils and immunity: challenges and opportunities. *Nat Rev Immunol* **6**, 173-182 (2006).
2. Coffelt, S.B., Wellenstein, M.D. & de Visser, K.E. Neutrophils in cancer: neutral no more. *Nat Rev Cancer* **16**, 431-446 (2016).
3. Templeton, A.J.*, et al.* Prognostic role of neutrophil-to-lymphocyte ratio in solid tumors: a systematic review and meta-analysis. *J Natl Cancer Inst* **106**, dju124 (2014).
4. Wei, B.*, et al.* The neutrophil lymphocyte ratio is associated with breast cancer prognosis: an updated systematic review and meta-analysis. *Onco Targets Ther* **9**, 5567-5575 (2016).
5. Gentles, A.J.*, et al.* The prognostic landscape of genes and infiltrating immune cells across human cancers. *Nat Med* **21**, 938-945 (2015).
6. Casbon, A.J.*, et al.* Invasive breast cancer reprograms early myeloid differentiation in the bone marrow to generate immunosuppressive neutrophils. *Proc Natl Acad Sci U S A* **112**, E566-575 (2015).
7. Coffelt, S.B.*, et al.* IL-17-producing gammadelta T cells and neutrophils conspire to promote breast cancer metastasis. *Nature* **522**, 345-348 (2015).
8. Sagiv, J.Y.*, et al.* Phenotypic diversity and plasticity in circulating neutrophil subpopulations in cancer. *Cell Rep* **10**, 562-573 (2015).
9. Yang, X.D.*, et al.* Histamine deficiency promotes inflammation-associated carcinogenesis through reduced myeloid maturation and accumulation of CD11b+Ly6G+ immature myeloid cells. *Nat Med* **17**, 87-95 (2011).
10. Chao, T., Furth, E.E. & Vonderheide, R.H. CXCR2-Dependent Accumulation of Tumor-Associated Neutrophils Regulates T-cell Immunity in Pancreatic Ductal Adenocarcinoma. *Cancer Immunol Res* **4**, 968-982 (2016).
11. Daley, J.M., Thomay, A.A., Connolly, M.D., Reichner, J.S. & Albina, J.E. Use of Ly6G-specific monoclonal antibody to deplete neutrophils in mice. *J Leukoc Biol* **83**, 64-70 (2008).
12. Fleming, T.J., Fleming, M.L. & Malek, T.R. Selective expression of Ly-6G on myeloid lineage cells in mouse bone marrow. RB6-8C5 mAb to granulocyte-differentiation antigen (Gr-1) detects members of the Ly-6 family. *J Immunol* **151**, 2399-2408 (1993).
13. Faget, J.*, et al.* Efficient and specific Ly6G+ cell depletion: A change in the current practices toward more relevant functional analyses of neutrophils. *biorxiv*, 498881 (2018).
14. Steele, C.W.*, et al.* CXCR2 Inhibition Profoundly Suppresses Metastases and Augments Immunotherapy in Pancreatic Ductal Adenocarcinoma. *Cancer Cell* **29**, 832-845 (2016).
15. Saintigny, P.*, et al.* CXCR2 expression in tumor cells is a poor prognostic factor and promotes invasion and metastasis in lung adenocarcinoma. *Cancer Res* **73**, 571-582 (2013).
16. Reber, L.L.*, et al.* Neutrophil myeloperoxidase diminishes the toxic effects and mortality induced by lipopolysaccharide. *J Exp Med* **214**, 1249-1258 (2017).
17. Rombouts, M.*, et al.* Long-Term Depletion of Conventional Dendritic Cells Cannot Be Maintained in an Atherosclerotic Zbtb46-DTR Mouse Model. *PLoS One* **12**, e0169608 (2017).
18. Wang, J., Siffert, M., Spiliotis, M. & Gottstein, B. Repeated Long-Term DT Application in the DEREG Mouse Induces a Neutralizing Anti-DT Antibody Response. *J Immunol Res* **2016**, 1450398 (2016).
19. Pajvani, U.B.*, et al.* Fat apoptosis through targeted activation of caspase 8: a new mouse model of inducible and reversible lipoatrophy. *Nat Med* **11**, 797-803 (2005).
20. Baker, D.J.*, et al.* Clearance of p16Ink4a-positive senescent cells delays ageing-associated disorders. *Nature* **479**, 232-236 (2011).
21. Rutkowski, J.M.*, et al.* Adiponectin promotes functional recovery after podocyte ablation. *J Am Soc Nephrol* **24**, 268-282 (2013).
22. Wang, Z.V.*, et al.* PANIC-ATTAC: a mouse model for inducible and reversible beta-cell ablation. *Diabetes* **57**, 2137-2148 (2008).
23. Srikrishna, G. S100A8 and S100A9: new insights into their roles in malignancy. *J Innate Immun* **4**,

31-40 (2012).
24. Derksen, P.W*., et al.* Somatic inactivation of E-cadherin and p53 in mice leads to metastatic lobular mammary carcinoma through induction of anoikis resistance and angiogenesis. *Cancer Cell* **10**, 437-449 (2006).
25. Doornebal, C.W*., et al.* A preclinical mouse model of invasive lobular breast cancer metastasis. *Cancer Res* **73**, 353-363 (2013).
26. Hiratsuka, S., Watanabe, A., Aburatani, H. & Maru, Y. Tumour-mediated upregulation of chemoattractants and recruitment of myeloid cells predetermines lung metastasis. *Nat Cell Biol* **8**, 1369-1375 (2006).
27. Dzhagalov, I., St John, A. & He, Y.W. The antiapoptotic protein Mcl-1 is essential for the survival of neutrophils but not macrophages. *Blood* **109**, 1620-1626 (2007).
28. Karsunky, H*., et al.* Inflammatory reactions and severe neutropenia in mice lacking the transcriptional repressor Gfi1. *Nat Genet* **30**, 295-300 (2002).
29. Ordonez-Rueda, D*., et al.* A hypomorphic mutation in the Gfi1 transcriptional repressor results in a novel form of neutropenia. *Eur J Immunol* **42**, 2395-2408 (2012).
30. Lieschke, G.J*., et al.* Mice lacking granulocyte colony-stimulating factor have chronic neutropenia, granulocyte and macrophage progenitor cell deficiency, and impaired neutrophil mobilization. *Blood* **84**, 1737-1746 (1994).
31. Cheng, P*., et al.* Inhibition of dendritic cell differentiation and accumulation of myeloid-derived suppressor cells in cancer is regulated by S100A9 protein. *J Exp Med* **205**, 2235-2249 (2008).
32. Lagasse, E. & Clerc, R.G. Cloning and expression of two human genes encoding calcium-binding proteins that are regulated during myeloid differentiation. *Mol Cell Biol* **8**, 2402-2410 (1988).
33. Dancey, J.T., Deubelbeiss, K.A., Harker, L.A. & Finch, C.A. Neutrophil kinetics in man. *J Clin Invest* **58**, 705-715 (1976).
34. Yuan, H*., et al.* MMTV-NeuT/ATTAC mice: a new model for studying the stromal tumor microenvironment. *Oncotarget* **9**, 8042-8053 (2018).
35. Lim, S.Y., Yuzhalin, A.E., Gordon-Weeks, A.N. & Muschel, R.J. Tumor-infiltrating monocytes/macrophages promote tumor invasion and migration by upregulating S100A8 and S100A9 expression in cancer cells. *Oncogene* **35**, 5735-5745 (2016).
36. Finisguerra, V*., et al.* MET is required for the recruitment of anti-tumoural neutrophils. *Nature* **522**, 349-353 (2015).
37. Huijbers, I.J*., et al.* Using the GEMM-ESC strategy to study gene function in mouse models. *Nat Protoc* **10**, 1755-1785 (2015).
38. Salvagno, C. & de Visser, K.E. Purification of Immune Cell Populations from Freshly Isolated Murine Tumors and Organs by Consecutive Magnetic Cell Sorting and Multi-parameter Flow Cytometry-Based Sorting. *Methods Mol Biol* **1458**, 125-135 (2016).

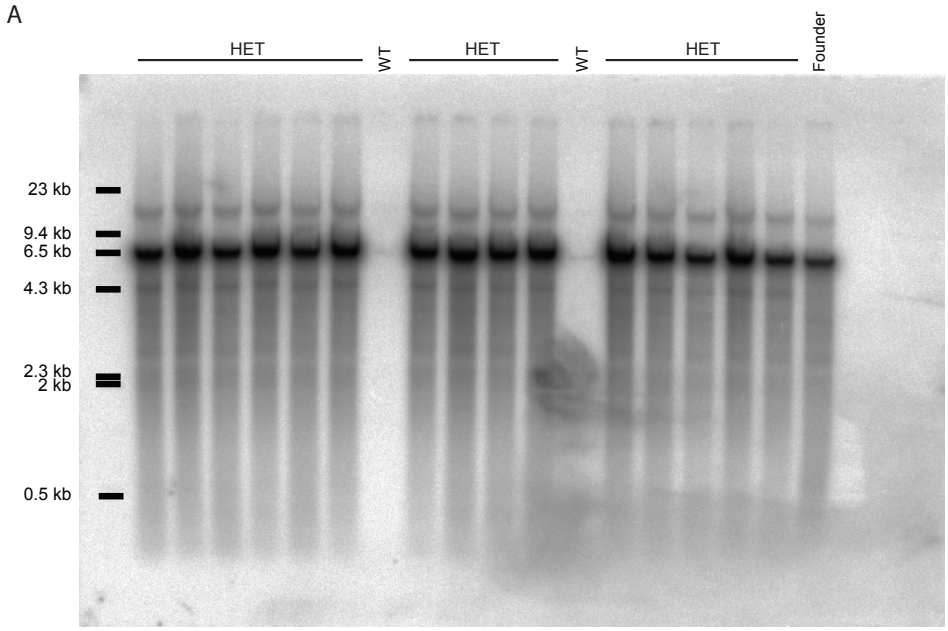


**Supplementary Fig. 1 | The hMRP8-ATTAC construct is integrated in one site in multiple copies.** (A) Southern Blot analysis of toe-derived genomic DNA of Founder 19, and heterozygous and WT F1 progeny. The transgene is identified by the hybridization of the GFP probe (concatamer band of 6114kb). HET, heterozygous. WT, wild-type

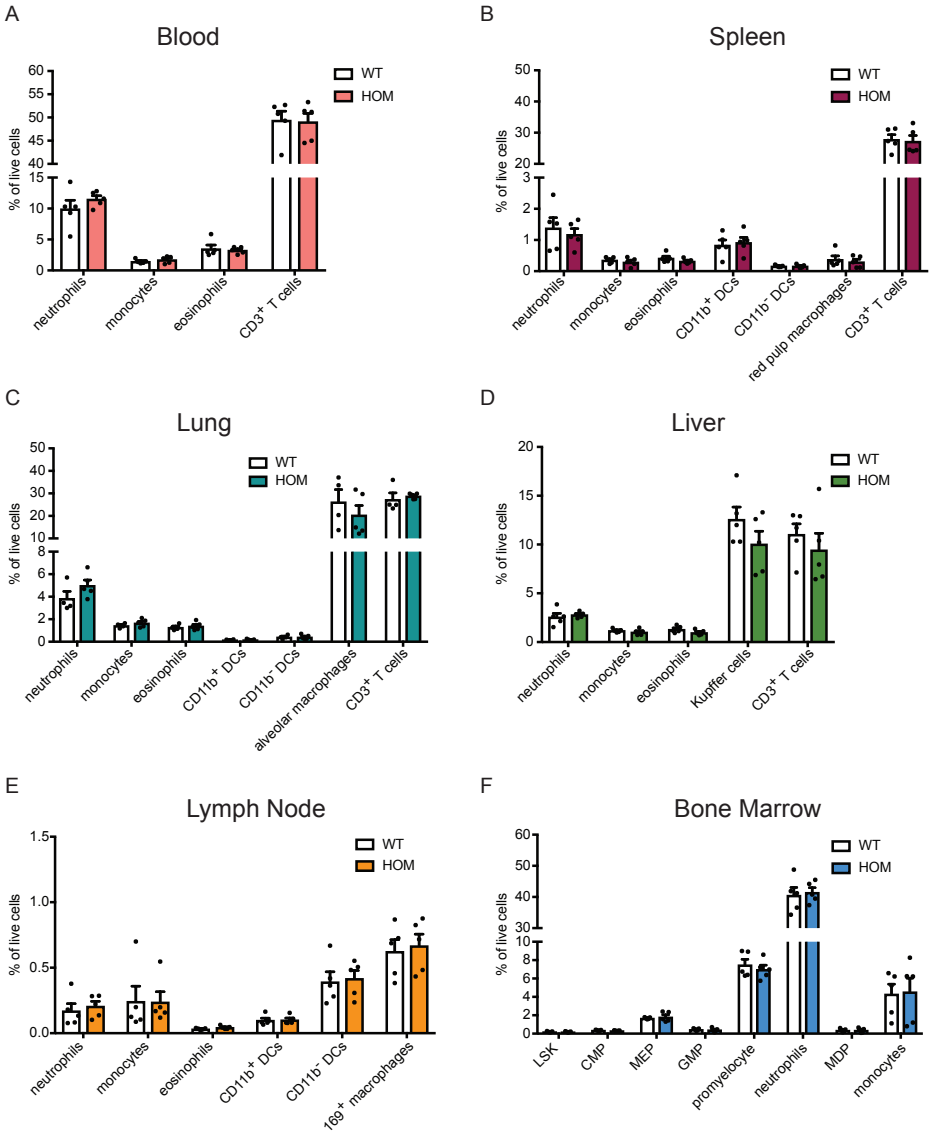


**Supplementary Fig. 2 | No changes in the immune cell composition in hMRP8-ATTAC mice.** (A-F) Immune cell proportion in the blood (A), spleen (B), lung (C), liver (D), lymph node (E) and bone marrow (F) of hMRP8-ATTAC mice and WT littermates (n=4-5). HOM, homozygous. Data are mean values ± SEM.

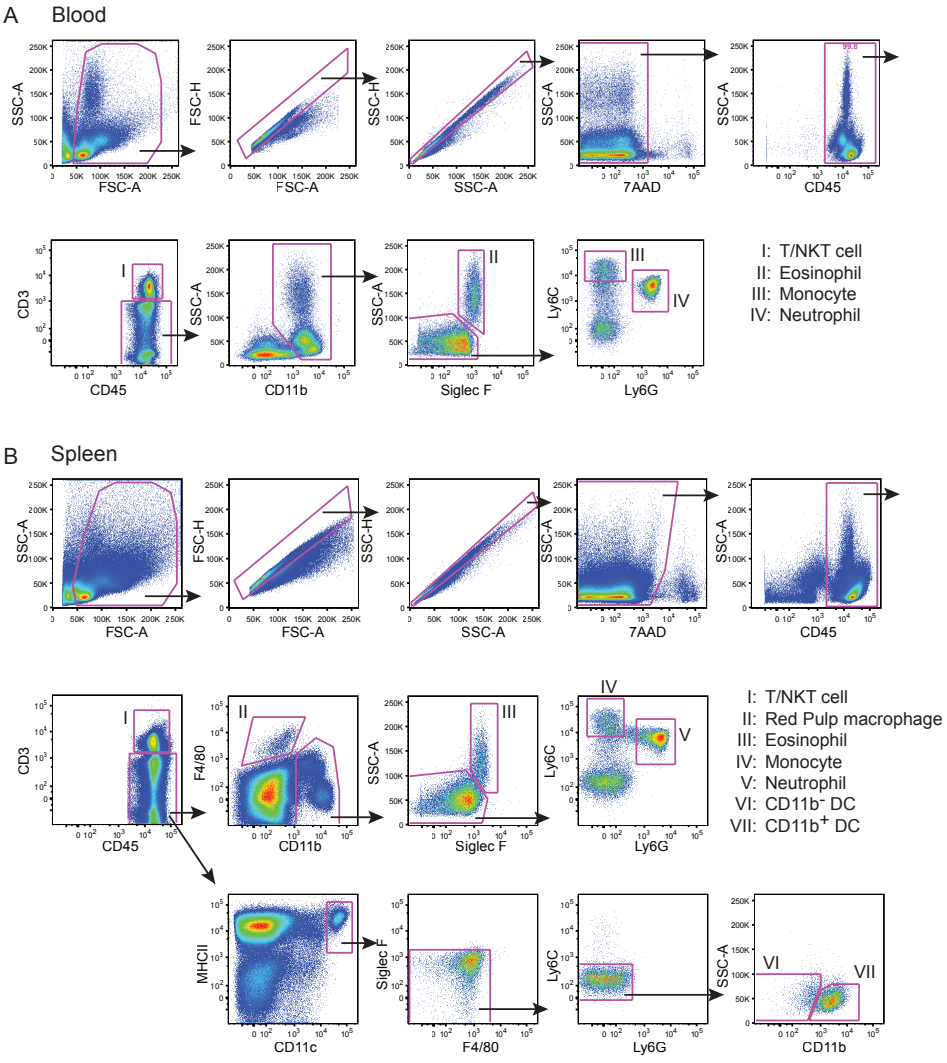


**Supplementary Fig. 3 | Flow cytometry gating strategy for blood and spleen samples.** (A-B) Representative dot plots of blood (A) and spleen (B) of a homozygous hMRP8-ATTAC mouse illustrating the gating strategy for the identification of cell populations. Antibody panel used: "Panel 1". Arrows indicate directionality of sub-gates.

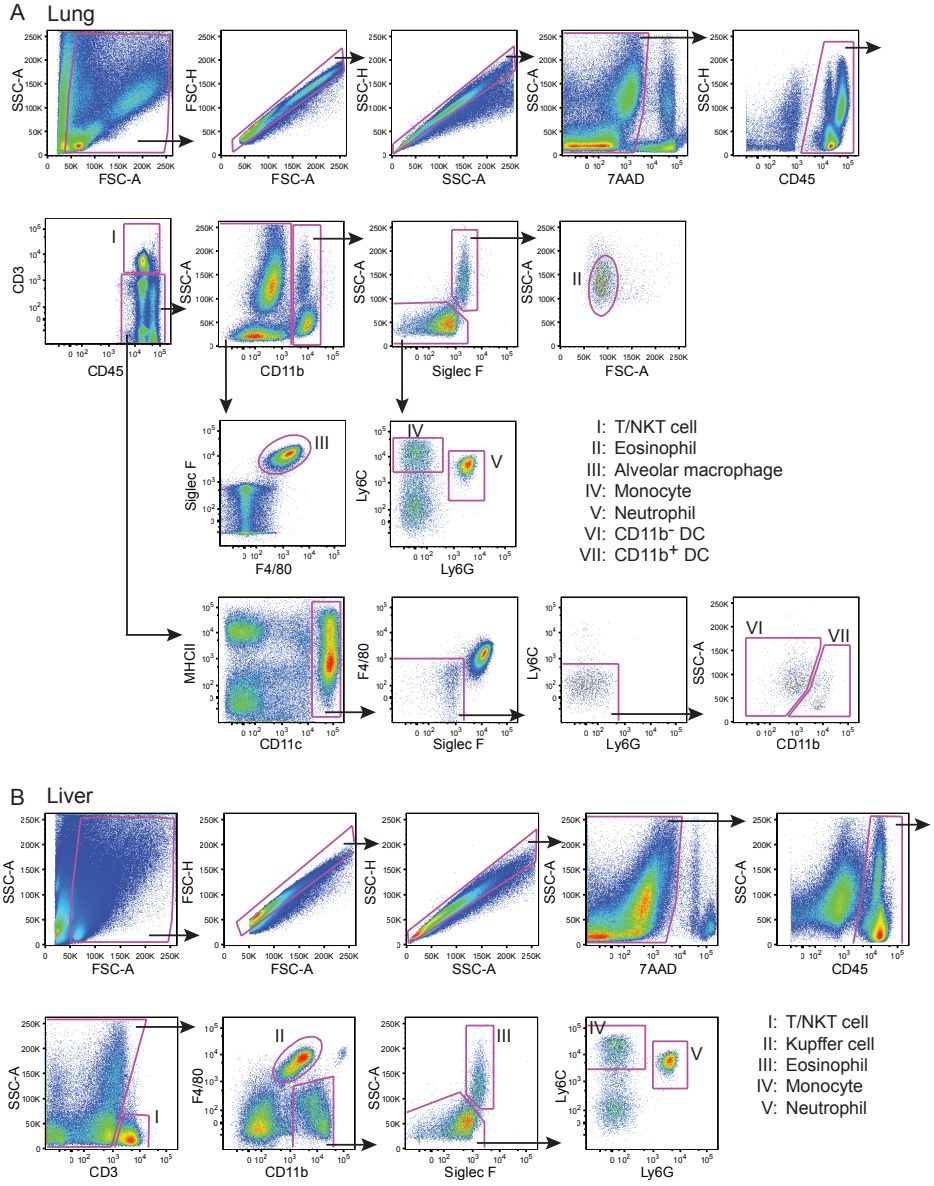


Supplementary Fig. 4 | Flow cytometry gating strategy for lung and liver samples. (A-B) Representative dot plots of lung (A) and liver (B) of a homozygous hMRP8-ATTAC mouse illustrating the gating strategy for the identification of cell populations. Antibody panel used: "Panel 1". Arrows indicate directionality of sub-gates.

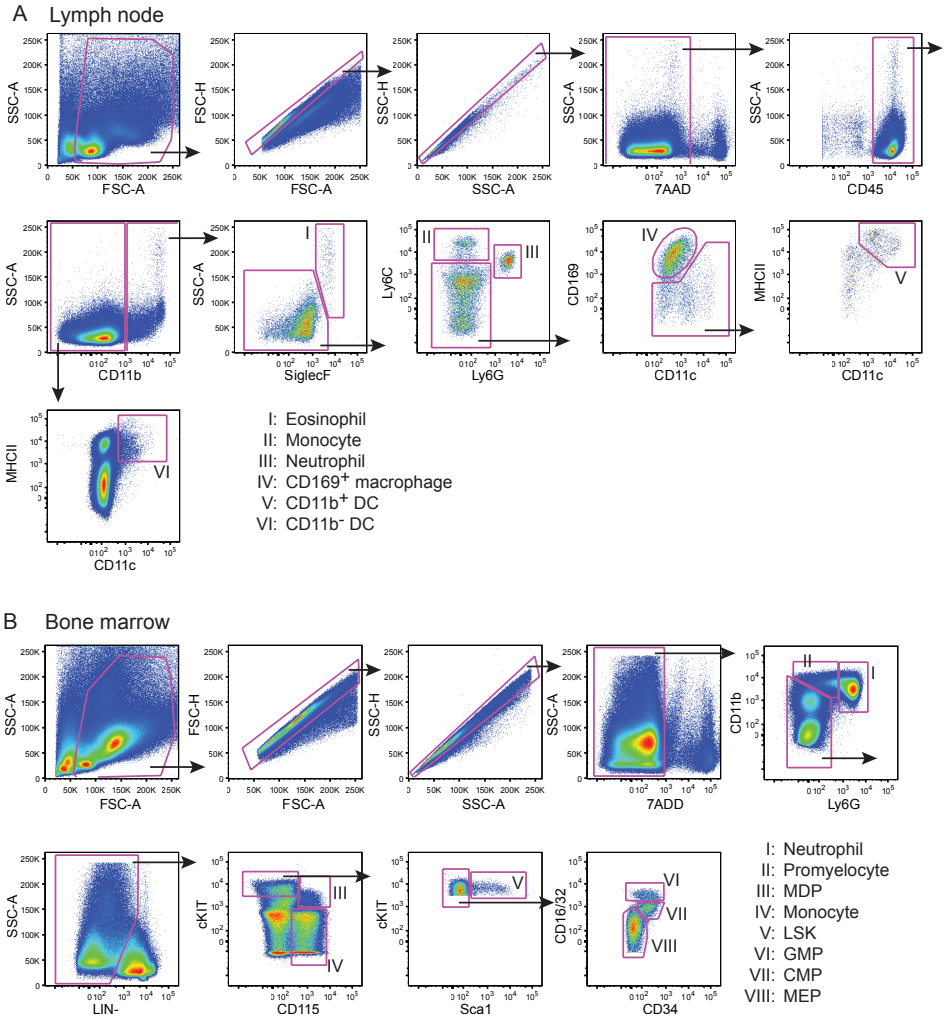


**Supplementary Fig. 5| Flow cytometry gating strategy for lymph node and bone marrow samples.** (A-B) Representative dot plots of lymph node (A) and bone marrow (B) of a homozygous hMRP8-ATTAC mouse illustrating the gating strategy for the identification of cell populations. Antibody panel used: "Panel 2" for lymph node and "Panel 3" for bone marrow. Arrows indicate directionality of sub-gates.

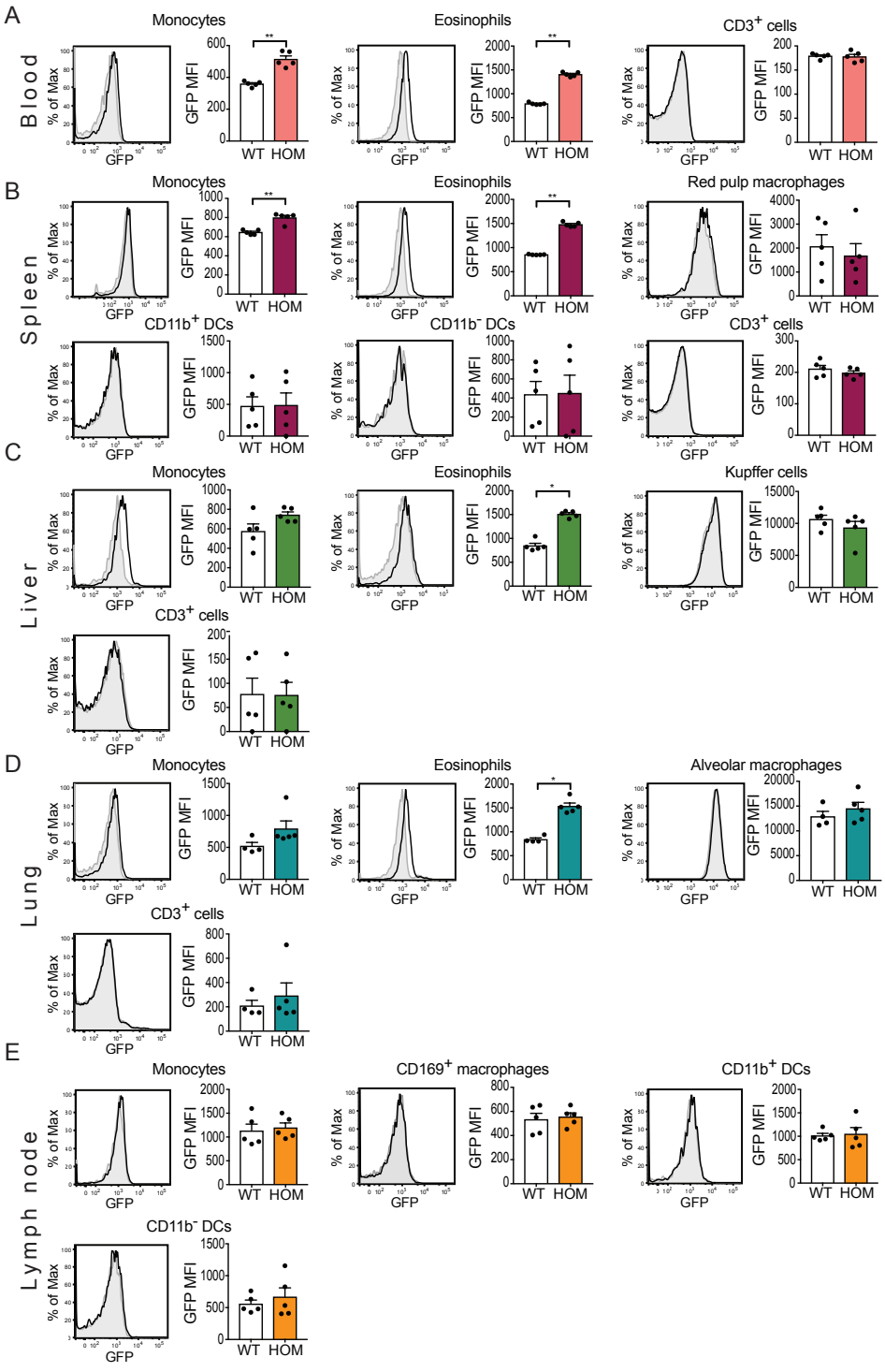
A
Blood
Monocytes
Eosinophils
CD3+ cells
B
Spleen
Monocytes
Eosinophils
Red pulp macrophages
CD11b+ DCs
CD11b- DCs
CD3+ cells
C
Liver
Monocytes
Eosinophils
Kupffer cells
CD3+ cells
D
Lung
Monocytes
Eosinophils
Alveolar macrophages
CD3+ cells
E
Lymph node
Monocytes
CD169+ macrophages
CD11b+ DCs
CD11b- DCs
% of Max
GFP
GFP MFI
WT HOM

**Supplementary Fig. 6 | Monocytes and eosinophils in the hMRP8-ATTAC model express low levels of the transgene.** (A-E) Representative histograms of GFP expression and quantification of the Median Fluorescence Intensity (MFI) of GFP in several immune cells from blood (A), spleen (B), liver (C), lung (D) and lymph node (E) of homozygous female hMRP8-ATTAC mice (n=5) compared to WT littermates (n=4-5), as determined by flow cytometry. WT, wild type; HOM, homozygous. Data are mean values ± SEM. *$p < 0.05$, **$p<0.01$ by Mann–Whitney test.

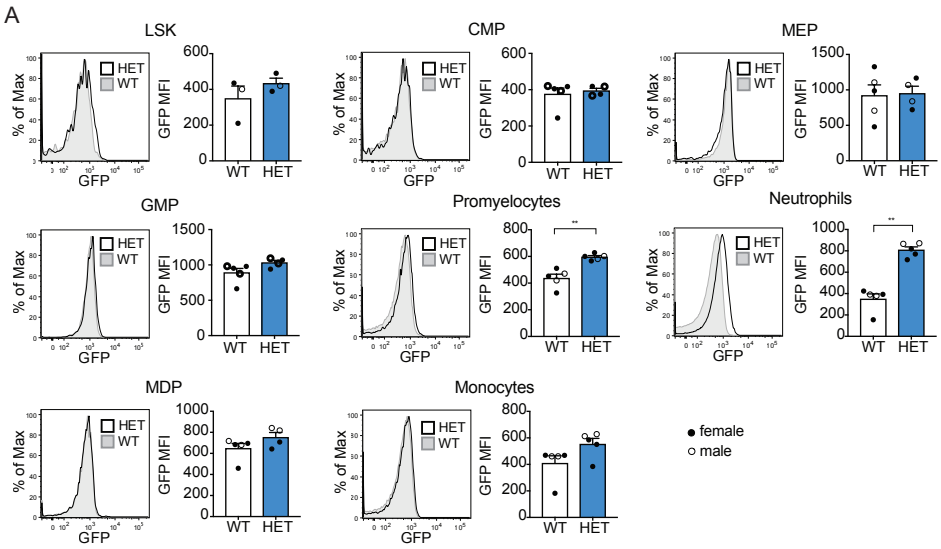


**Supplementary Fig. 7 | GFP expression in the bone marrow of heterozygous hMRP8-ATTAC mice.** (A) Representative histograms of GFP expression and quantification of the Median Fluorescence Intensity (MFI) of GFP in different hematopoietic cell populations depicted in Fig. 3A in the bone marrow of heterozygous hMRP8-ATTAC mice (n=3-5) and WT littermates (n=3-5), as determined by flow cytometry. Open circles represent male hMRP8-ATTAC mice and full circles represent female hMRP8-ATTAC mice. WT, wild type; HET, heterozygous. LSK, Lineage-SCA1+Kit-; CMP, common myeloid progenitor; MEP, megakaryocyte-erythroid progenitor; GMP, granulocyte-macrophage progenitor; MDP, monocyte/macrophage-dendritic cell progenitor. Data presented are mean values ± SEM. **p<0.01 by Mann–Whitney test.

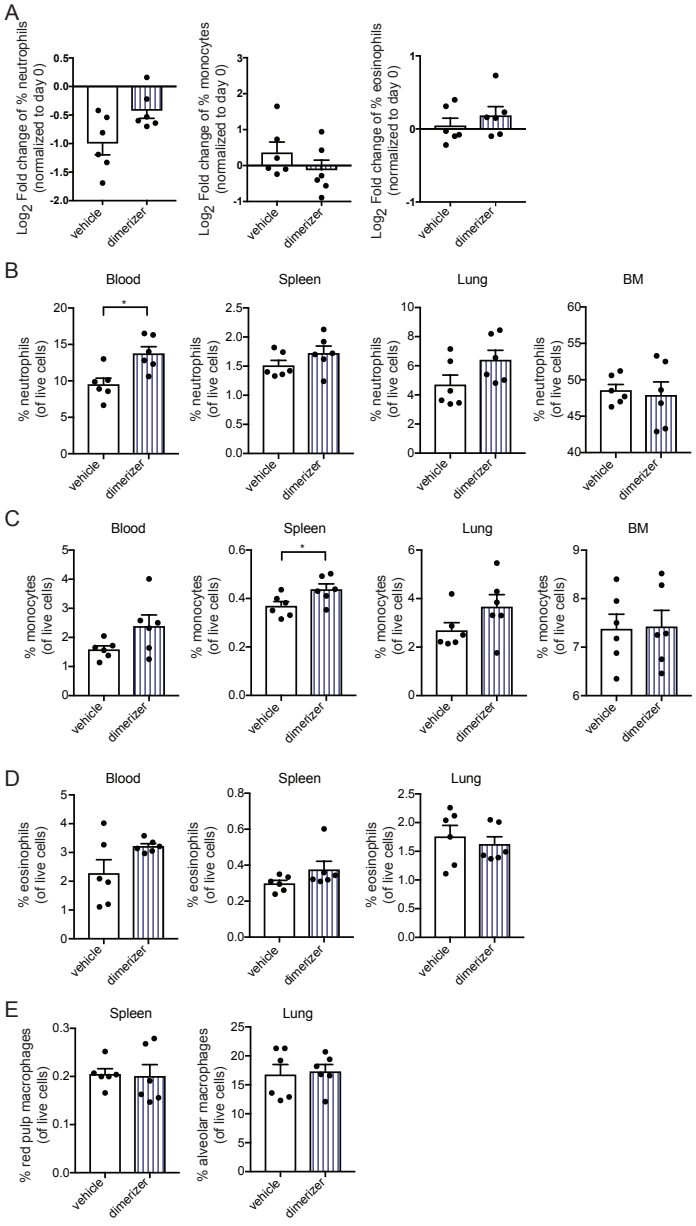


**Supplementary Fig. 8 | Dimerizer treatment has modest effects on neutrophils in WT mice.** (A) Log2 fold change of circulating neutrophils, monocytes and eosinophils defined as % of live two days after treatment compared to day 0 in WT female mice (n=6/group). Fold change was calculated by dividing the frequency of neutrophil at day 2 by the frequency of neutrophils at day 0. (B-E) Frequencies of neutrophils (B), monocytes (C), eosinophils (D) and resident macrophages (E) in blood, spleen, lung and bone marrow of WT mice treated with vehicle or dimerizer for seven consecutive days, as determined by flow cytometry (n=6/group, same mice as in A). Data are mean values ± SEM. *$p < 0.05$ by Mann–Whitney test.

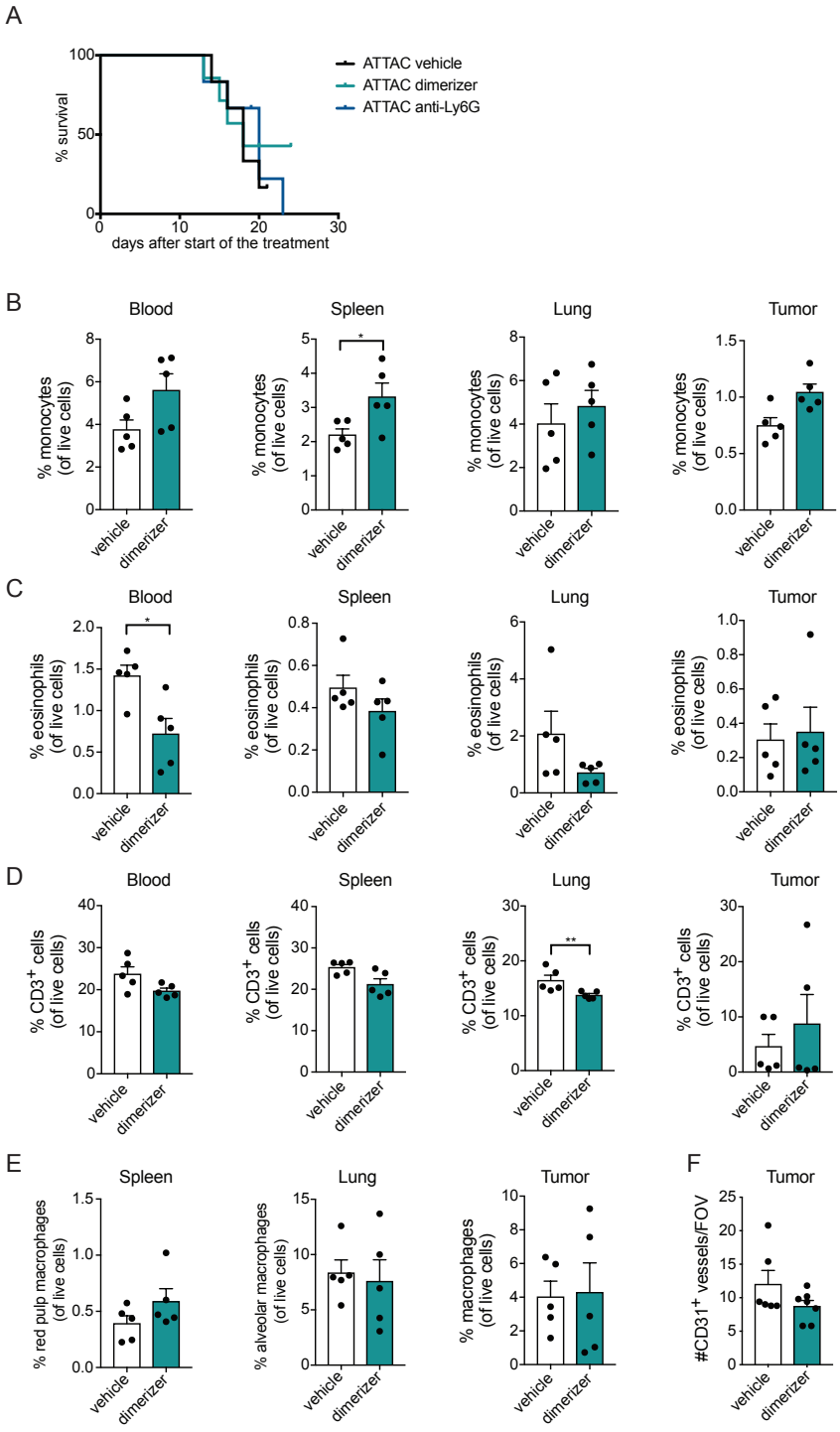
A
% survival
days after start of the treatment
ATTAC vehicle
ATTAC dimerizer
ATTAC anti-Ly6G
B
Blood
Spleen
Lung
Tumor
% monocytes (of live cells)
C
% eosinophils (of live cells)
D
% CD3+ cells (of live cells)
E
% red pulp macrophages (of live cells)
% alveolar macrophages (of live cells)
% macrophages (of live cells)
F
#CD31+ vessels/FOV
vehicle
dimerizer

**Supplementary Fig. 9 | Dimerizer treatment slightly increases monocyte frequency and reduces circulating eosinophils in tumor-bearing hMRP8-ATTAC mice.** (A) Kaplan-Meier tumor-specific survival curves of hMRP8-ATTAC mice treated with vehicle (n=6), dimerizer (n=7) or anti-Ly6G (n=6). An event is defined as an animal with a tumor size of 225mm$^2$. (B-E) Frequency of monocytes (B), eosinophils (C), CD3$^+$ T cells (D) and macrophages (E) in the blood, spleen, lung and tumor of end-stage tumor-bearing hMRP8-ATTAC mice (n=5/group), as determined by flow cytometry. (F) Quantification of CD31$^+$ vessels in viable areas of mammary tumors in hMRP8-ATTAC mice treated as indicated (n=6-7). Data are mean values ± SEM. *$p < 0.05$, **$<0.01$ by Mann–Whitney test.

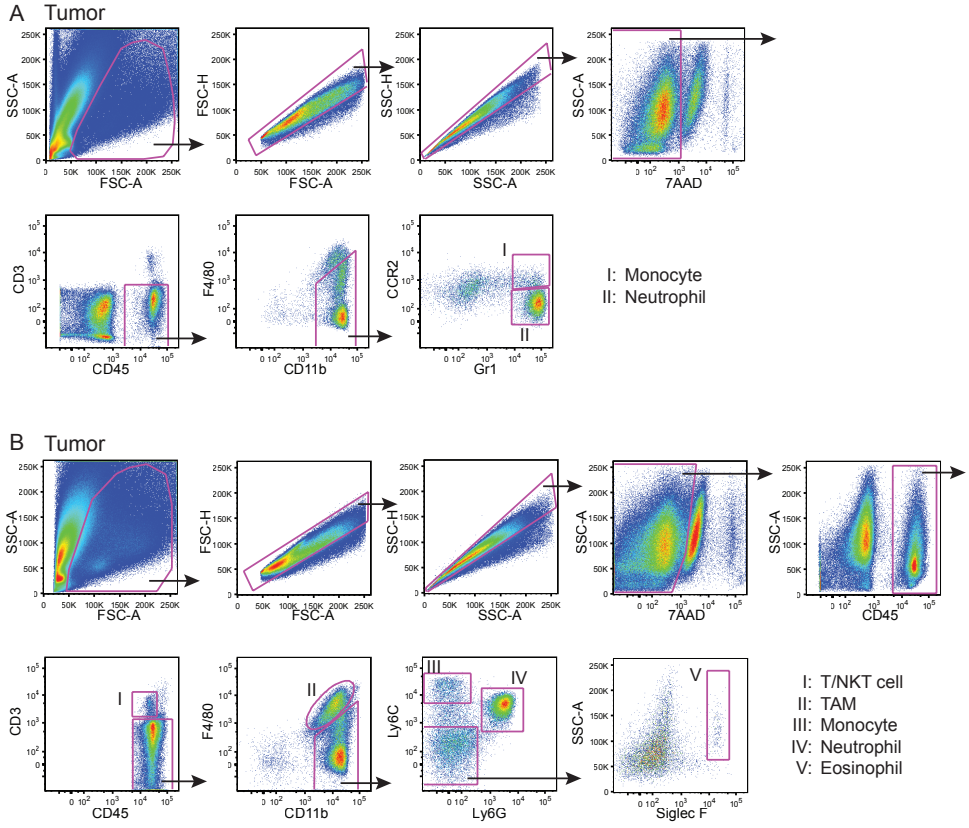


**Supplementary Fig. 10 | Flow cytometry gating strategy for tumor samples.** (A-B) Representative dot plots of tumor samples of a homozygous hMRP8-ATTAC mouse orthotopically transplanted with *K14cre;Cdh1$^{F/F}$;Trp53$^{F/F}$* mammary tumor piece illustrating two gating strategies for the identification of cell populations. Antibody panel used: "Panel 4" in (A) and "Panel 5" in (B). Arrows indicate directionality of sub-gates. (A) was used in Fig. 5E to identify neutrophils.

Supplementary Table 1: List of antibodies used for flow cytometry analyses.

Panel 1. Blood, spleen, lung and liver

| Antibody | Fluorophore | Clone | Vendor | Dilution |
|---|---|---|---|---|
| CD45 | BUV395 | 30-F11 | BD Biosciences | 1:200 |
| CD3 | PE-cy7 | 145-2c11 | eBioscience | 1:200 |
| Siglec F | BV605 | E50-2440 | BD Biosciences | 1:200 |
| CD11b | BV786 | M1/70 | BD Biosciences | 1:400 |
| CD11c | PE | N418 | eBioscience | 1:200 |
| Ly6G | AF700 | 1A8 | Biolegend | 1:200 |
| Ly6C | Ef450 | HK1.4 | eBioscience | 1:400 |
| F4/80 | APC | BM8 | eBioscience | 1:200 |
| MHC class II | APCef780 | M5/114.15.2 | eBioscience | 1:200 |

Panel 2. Lymph node

| Antibody | Fluorophore | Clone | Vendor | Dilution |
|---|---|---|---|---|
| CD45 | BUV395 | 30-F11 | BD Biosciences | 1:200 |
| Siglec F | BV605 | E50-2440 | BD Biosciences | 1:200 |
| CD11b | BV786 | M1/70 | BD Biosciences | 1:400 |
| CD11c | BV421 | HL3 | BD Biosciences | 1:200 |
| Ly6G | AF700 | 1A8 | Biolegend | 1:200 |
| Ly6C | PEcy7 | HK1.4 | Biolegend | 1:400 |
| F4/80 | APC | BM8 | eBioscience | 1:200 |
| MHC class II | APCef780 | M5/114.15.2 | eBioscience | 1:200 |
| CD169 | PE | 3D6.112 | Biolegend | 1:200 |

Panel 3. Bone marrow

| Antibody | Fluorophore | Clone | Vendor | Dilution |
|---|---|---|---|---|
| CD11b | APCef780 | M1/70 | eBioscience | 1:400 |
| CD115 | BV711 | AFS98 | Biolegend | 1:200 |
| Ly6G | AF700 | 1A8 | Biolegend | 1:200 |
| Ter119 | PE | TER-119 | Biolegend | 1:400 |
| CD3 | PE | 145-2C11 | Biolegend | 1:400 |
| CD4 | PE | H129.19 | Biolegend | 1:400 |
| CD8 | PE | 53-6.7 | eBioscience | 1:400 |
| CD19 | PE | eBio1D3 | eBioscience | 1:400 |
| Sca1 | BV421 | D7 | Biolegend | 1:400 |
| CD117 | BV605 | 2B8 | BD Biosciences | 1:200 |
| CD16/32 | BUV395 | 2.4G2 | BD Biosciences | 1:200 |
| CD34 | AF647 | RAM34 | BD Biosciences | 1:100 |

Panel 4. Dimerizer treatment in tumor-bearing hMRP8;ATTAC mice: blood, spleen, lung and tumor

| Antibody | Fluorophore | Clone | Vendor | Dilution |
|---|---|---|---|---|
| CD45 | BUV395 | 30-F11 | BD Biosciences | 1:200 |
| CD3 | PE-cy7 | 145-2c11 | eBioscience | 1:200 |
| CD11b | BV786 | M1/70 | BD Biosciences | 1:400 |
| CCR2 | PE | 475301 | R&D systems | 1:100 |
| Gr1 | BV421 | RB6-8C5 | Biolegend | 1:200 |
| F4/80 | APC | BM8 | eBioscience | 1:200 |

Panel 5. Dimerizer treatment in tumor-bearing hMRP8;ATTAC mice: blood, spleen, lung and tumor

| Antibody | Fluorophore | Clone | Vendor | Dilution |
|---|---|---|---|---|
| CD45 | BUV395 | 30-F11 | BD Biosciences | 1:200 |
| CD3 | PE-cy7 | 145-2c11 | eBioscience | 1:200 |
| Siglec F | PE | E50-2440 | BD Biosciences | 1:200 |
| CD11b | BV786 | M1/70 | BD Biosciences | 1:400 |
| CD11c | BUV737 | HL3 | BD Biosciences | 1:100 |
| CD117 | BV605 | 2B8 | BD Biosciences | 1:100 |
| Ly6G | AF700 | 1A8 | Biolegend | 1:200 |
| Ly6C | Ef450 | HK1.4 | eBioscience | 1:400 |
| F4/80 | APC | BM8 | eBioscience | 1:200 |
| MHC class II | APCef780 | M5/114.15.2 | eBioscience | 1:200 |